AFRL-HE-WP-TP-2006-0015

AIR FORCE RESEARCH LABORATORY

Ultrabright Head Mounted Displays Using LED-Illuminated LCOS

M. A. Handschy
J. R. McNeil
P. E. Weissman

Displaytech, Inc.
2602 Clover Basin Drive
Longmont CO 80503

January 2006

20060322007

Human Effectiveness Directorate
Warfighter Interface Division
Wright-Patterson AFB OH 45433

REPORT DOCUMENTATION PAGE

Form Approved OMB No. 0704-0188

1. REPORT DATE *(DD-MM-YYYY)*
January 2006

2. REPORT TYPE
Conference Proceedings

3. DATES COVERED *(From - To)*

4. TITLE AND SUBTITLE
Ultrabright Head Mounted Displays Using LED-Illuminated LCOS

5a. CONTRACT NUMBER

5b. GRANT NUMBER

5c. PROGRAM ELEMENT NUMBER

6. AUTHOR(S)
M. A. Handschy, J. R. McNeil, P. E. Weissman

5d. PROJECT NUMBER
3005

5e. TASK NUMBER
HC

5f. WORK UNIT NUMBER
52

7. PERFORMING ORGANIZATION NAME(S) AND ADDRESS(ES) AND ADDRESS(ES)
Displaytech, Inc.
2602 Clover Basin Drive
Longmont CO 80503

8. PERFORMING ORGANIZATION REPORT NUMBER

9. SPONSORING / MONITORING AGENCY NAME(S) AND ADDRESS(ES)
Air Force Materiel Command
Air Force Research Laboratory
Human Effectiveness Directorate
Warfighter Interface Division
Wright-Patterson AFB OH 45433-7022

10. SPONSOR/MONITOR'S ACRONYM(S)
AFRL/HECV

11. SPONSOR/MONITOR'S REPORT NUMBER(S)
AFRL-HE-WP-TP-2006-0015

12. DISTRIBUTION / AVAILABILITY STATEMENT
Approved for public release; distribution is unlimited. Clearance AFRL/WS-06-0258, 2 Feb 06.

13. SUPPLEMENTARY NOTES
This will be published in the SPIE Helmet- and Head-Mounted Displays conference proceedings. The clearance number is AFRL/WS-06-0258, cleared 2 February 2006.

14. ABSTRACT
We report design and test of a high brightness laboratory-breadboard LED/LCOS HMD system employing a 0.78-inch-diagonal 1280 x 768 ferroelectric liquid-crystal-on-silicon microdisplay and a red-green-blue LED. With an 8x viewing optic giving a 35 degree diagonal field of view, the system yielded brightnesses greater 40,000 cd/m2 (12,000 fL) in color-sequential mode and greater than 100,000 cd/m2 (30,000 fL) in monochrome mode, at LED power consumptions of 1.1 W and 3.3 W, respectively. The illumination optics employed a rectangular light pipe and tailored diffuser to efficiently fill the microdisplay panel aperture and exit pupil. The high efficiency of such image generators facilities display readability in see-through HMDs operating in high-ambient-light environments, as well as enabling ultra-low power HMDs (less than 100 mW total) for dismounted users of battery-powered systems.

15. SUBJECT TERMS
Helmet mounted display, HMD, liquid crystal on silicon, LCOS, light emitting diode, LED

16. SECURITY CLASSIFICATION OF: Unclassified			17. LIMITATION OF ABSTRACT	18. NUMBER OF PAGES	19a. NAME OF RESPONSIBLE PERSON
a. REPORT	b. ABSTRACT	c. THIS PAGE			Douglas Franck
UNC	UNC	UNC	SAR	12	19b. TELEPHONE NUMBER *(include area code)* (937) 656-7108

Standard Form 298 (Rev. 8-98)
Prescribed by ANSI Std. 239.18

Ultrabright Head Mounted Displays Using LED-Illuminated LCOS

Mark A. Handschy and John R. McNeil
Displaytech, Inc., 2602 Clover Basin Dr., Longmont, CO, USA 80503
Paul E. Weissman
Optical Resolutions, Inc., 155 E. Main St., Suite 308, Brewster, NY 10509

ABSTRACT

We report design and test of a high brightness laboratory-breadboard LED/LCOS HMD system employing a 0.78-inch-diagonal 1280 × 768 ferroelectric liquid-crystal-on-silicon microdisplay and a red-green-blue LED. With an 8× viewing optic giving a 35°-diagonal field of view, the system yielded brightnesses greater 40,000 cd/m^2 (12,000 fL) in color-sequential mode and greater than 100,000 cd/m^2 (30,000 fL) in monochrome mode, at LED power consumptions of 1.1 W and 3.3 W, respectively. The illumination optics employed a rectangular light pipe and tailored diffuser to efficiently fill the microdisplay panel aperture and exit pupil. The high efficiency of such image generators facilitates display readability in see-through HMDs operating in high-ambient-light environments, as well as enabling ultra-low power HMDs (less than 100 mW total) for dismounted users of battery-powered systems.

Keywords: helmet mounted display, HMD, liquid crystal on silicon, LCOS, light emitting diode, LED

1. INTRODUCTION

The emergence of high-brightness light-emitting diodes (LEDs) and liquid-crystal-on-silicon (LCOS) microdisplays promises a new generation of image generators for head mounted displays (HMDs). These HMDs would offer a wide spectrum of performance capabilities: at one end, ultra-low power operation (less than 100 mW total) for dismounted users of battery-powered systems – at the other end, ultra-high brightness (greater than 10,000 fL) to ensure contrast of displayed imagery against see-through full-daylight background scenes in aircraft cockpits. LED/LCOS image generators operate at low voltages, and facilitate integration of system electronics into the LCOS backplane to permit standard video interfaces with few-wire interconnects and on-chip programmable display gamma and scalable image formatting.

In addition to facilitating readability for see-through HMDs operating in high-ambient environments, the high brightness of such image generators enables novel HMD optical systems with better correction and larger fields of view and exit pupils than would otherwise be available with small LCOS microdisplay diagonals.

2. FUNDAMENTAL CONSIDERATIONS

Unlike the situation with emissive displays, the separation of the illumination components from the display panel in an LCOS display allows the overall system to be optimized for optical efficiency without compromising image performance. Consider the model HMD system diagramed in Figure 1. The effective focal length f of the viewing optics is chosen to give the desired field of view (FOV) for a chosen display panel diagonal d_{FLC}: $\tan\theta_{\mathrm{FOV}} = d_{\mathrm{FLC}}/(2f)$. Light from the illuminator should, at every point on the panel, fill a cone of half-angle θ_{FLC} sufficient to fill the viewing box or exit pupil of diameter d_{exit}: $\tan\theta_{\mathrm{FLC}} = d_{\mathrm{exit}}/(2f)$ Independent of the particulars of the optical design, important geometrical principles affect its efficiency. If the light source has area A_{LED}, and emits light into a cone of half-angle θ_{LED}, while the viewing box has area A_{exit} =

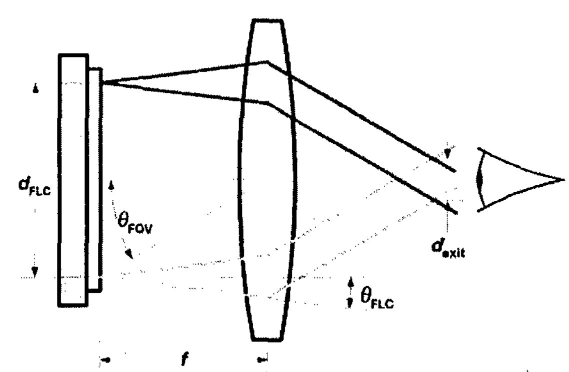

Figure 1. Basic microdisplay HMD geometry.

$\pi d^2_{exit}/4$, and the display image subtends an angle $2\theta_{FOV}$, then efficient use of the light source requires

$$A_{LED} < A_{exit} \sin^2\theta_{FOV}/\sin^2\theta_{LED}. \quad (1)$$

For an exit pupil diameter of 12 mm and a display FOV of 60° (θ_{FOV} = 30°), the largest useful lambertian (θ_{LED} = 90°) light source would have an area of 28 mm^2. According to the brightness theorem, a larger light source would necessarily result in wasted light. The fact that the field of view is typically rectangular rather than round further reduces the useful source area. The parameters in this example indicate the light source should have a spatial extent of a few millimeters (e.g. 5.3 mm if square in this example), consonant with the sizes of high-brightness LED die.

3. ILLUMINATION SYSTEM DESIGN

We constructed a breadboard system, as shown in Figure 2, modeled after a microdisplay projection display system. The OSTAR light source (Osram Opto Semiconductors GmbH, Regensburg) comprises four 1 mm × 1 mm LED die (two green, one red, and one blue) spaced by 0.1 mm to give a 2.1 mm square array. Table 1 gives the source characteristics. The LED source emits into a tapered acrylic integrator rod, similar to that described by Kuhn *et al.*,[1] that collects and homogenizes the light. Our integrator rod had a length of 52 mm, with a 2.4 mm × 2.4 mm square entrance face and a 9.3 mm × 5.6 mm rectangular output face. The rod output face was imaged through a polarizing beam splitter (PBS) of 25-mm cross section onto the 16.9 mm × 10.1 mm active area of the 1280 × 768 ferroelectric liquid crystal on silicon microdisplay panel (Displaytech, Inc.) by a 1.7× relay lens system comprising a fast aspheric condenser and a plano-convex doublet. The output face of the integrator rod was placed at the focal point of the condenser lens which then produces a real image of the LED die in the plane of an iris, the iris itself being at the focal point of the PCX doublet. With this arrangement the principal illumination rays are perpendicular to the face of the LCOS microdisplay panel. An 8× magnifier loupe (Peak Optics) designed for viewing of 35 mm film frames gave a 35°-diagonal field of view of the display panel active area and produced a de-magnified real image of the iris about 30 mm above the last surface of the magnifier.

	UNITS	RED	GREEN	BLUE
dominant wavelength	nm	617	525	464
drive current	mA	750	500	500
forward voltage	V	2.9	3.5	3.5
luminous intensity	cd	18	28	3.5
luminous flux	lm	55	86	10.5
efficacy	lm/W	25	25	6

Table 1. LED characteristics. Manufacturer's data sheet typical values.

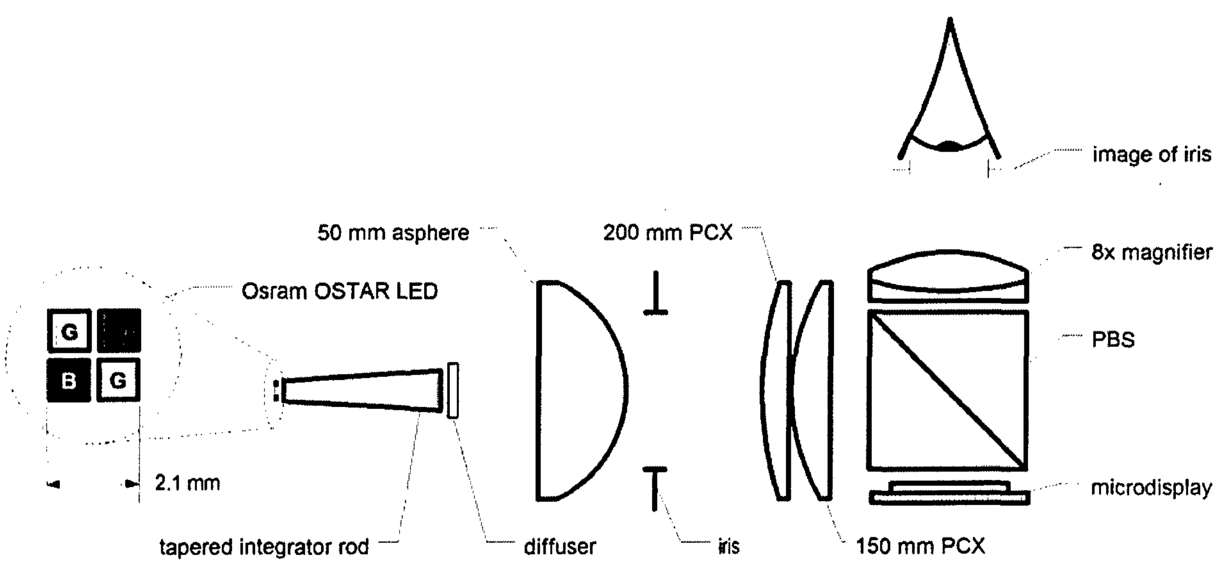

Figure 2. High-brightness HMD optical bread board schematic, including focal lengths for plano-convex (PCX) and aspheric lenses (not to scale).

4. RESULTS

With the OSTAR source inside an integrating sphere, we adjusted the LED drive currents while measuring CIE color coordinates with a Minolta CS-100 spot meter pointed into the sphere opening. The drive conditions listed in Table 2 gave white light with x-y color coordinates (0.318, 0.327), close to the color of a 6000 K black body, as shown in Figure 3 which also shows the color coordinates of the red, green, and blue LED-illuminator primaries. Luminous flux was measured with the OSTAR in the integrating sphere opening with a black paper aperture surrounding the LED emitting surface. After measuring the efficiency of the bare source we aligned it with the integrating rod by observing the LED image in the plane of the iris in Figure 2. The total internal reflection at the rod walls produces a kaleidoscope-like image, as shown in Figure 5(a); when the 2.1-mm LED source is centered in the 2.4-mm entrance face of the rod, the width of all the dark lines between repeated LED images is equal (to 0.15 mm). Luminous flux measured with the output end of the rod in the integrating sphere opening reaches a maximum when the input face of the rod touches the encapsulant on top of the LED die. Under these conditions we obtained 10–11 lm, giving a coupling efficiency of 57–63%, with the lower value being more representative of the conditions under which subsequent measurements were made.

Aligning the panel active area to the image of the integrator-rod output face gave a uniformly illuminated display image viewed through the 8× magnifier. However, the kaleidoscope pattern of Figure 5(a) appears at the nominal position of the viewer's eye, resulting in small shifts in the apparent color of the display image with small lateral shifts in eye position. By evaluating three diffusers of various strengths (Wavefront Technologies, Paramount, CA) placed over the output face of the integrator rod we found this problem could be rectified without significant loss of brightness. The diffuser angular characteristics in Figure 4 were measured by illuminating each diffuser at normal incidence with a laser beam of about 1 mm diameter, and measuring the irradiance E about one meter from the diffuser sample as a function of angle θ away from the incident beam. For diffuser I we normalized the on-axis irradiance $E_I(\theta = 0)$ to 1; for diffusers II and III we normalized E_{II} and E_{III} by the relative scale factors shown in Figure 4 to facilitate comparison. Figure 5 shows the exit-pupil uniformity improvement produced by the various diffusers. From the end of the 52-mm integrator rod, the LEDs on 1.1-mm centers subtend 1.2°. Diffuser III, with an angular half-width at half-maximum (HWHM) a few times greater than the LED separation is sufficient to yield an essentially uniform exit pupil.

Table 3 lists display brightnesses measured for various diffuser strengths and LED drive conditions. Measurements were made with a spot meter centered in the light beam leaving the display, and pointed at the center of the display but focused on the image

	UNITS	RED	GRN	BLUE	WHITE
LED current	mA	550	500	424	
LED voltage	V	2.74	6.78	3.53	
LED power	mW	250	570	250	1070
flux	lm				17.5
efficacy	lm/W				16.4

Table 2. LED source operating conditions. Power and flux under 1/6 duty cycle color-sequential drive.

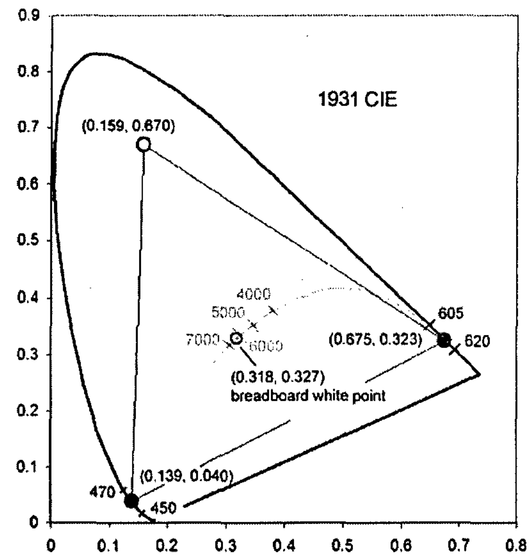

Figure 3. Primary and white-point color coordinates,

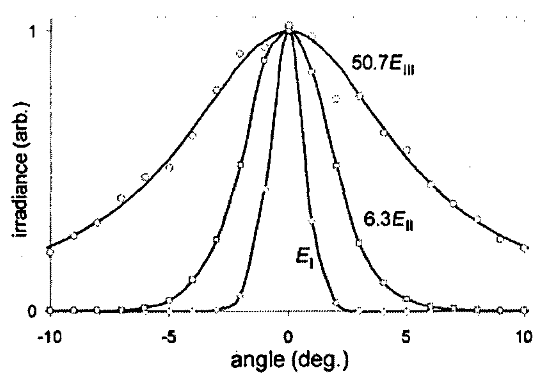

Figure 4. Diffuser angular characteristics.

DIFFUSER	BRIGHNTESS (NIT)		HWHM
	1/6 DUTY	1/2 DUTY	(DEG.)
none	60 800	157 300	0.0
I	54 100	147 700	0.9
II	54 600	142 300	2.1
III	40 300	105 200	5.5

Table 3. Display brightness.

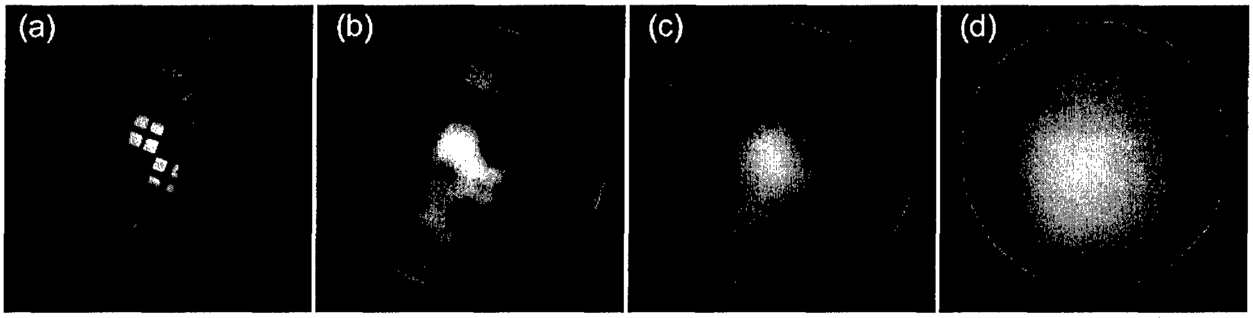

Figure 5. Exit pupil appearance for various diffuser strengths: (a) no diffuser, (b), (c), (d) diffusers I, II, III. The iris image is 11 mm in diameter.

Figure 6. Display images as viewed through the 8× magnifier. The photos show an approximately XGA (1024 × 768) portion of the 1280 × 768 display active area due to limitations of the camera lens angle.

of the iris. The 1/6 duty-cycle measurements correspond to achievable brightness in color-sequential operation, while the 1/2 duty-cycle values correspond to black-and-white operation. Insertion of a diffuser of strength sufficient to give an essentially uniform exit pupil produced only a modest brightness loss. Figure 6 shows the appearance of the display operated in color-sequential mode as seen through the magnifier. The wide color gamut of the LED illuminator gives vivid, well-saturated colors. Field curvature of the simple magnifier viewing optic results in loss of focus sharpness away from the center of the field in the photographs.

LED illuminators enable display dimming over very wide brightness ranges using pulse width modulation (PWM) drive. Figure 7(a) shows the variation of OSTAR light output vs. drive duty cycle at the same currents listed in Table 2. Variation was limited to approximately three orders of magnitude by the 5 μs rise time of the laboratory current source used to drive the LEDs; greater dimming ranges could be had with simple improvements. PWM dimming produces very little color shift, as shown by the color trajectory of Figure 7(b).

5. DISCUSSION

The projector-type illumination system of Figure 2 efficiently conveys light from the source to the panel to the exit pupil without unnecessary geometrical losses—i.e., it allows the spatial extent of the microdisplay panel to be uniformly filled (but not unnecessarily overfilled) with light of an angular distribution that just fills (but doesn't overfill) the exit pupil. The remaining losses in such a system arise principally from polarization and reflection terms listed in Table 4. Although LCOS microdisplays typically require polarized light, the geometrical considerations of equation (1) allow sources larger than e.g. the OSTAR used here without loss of efficiency. Thus, polarization conversion systems

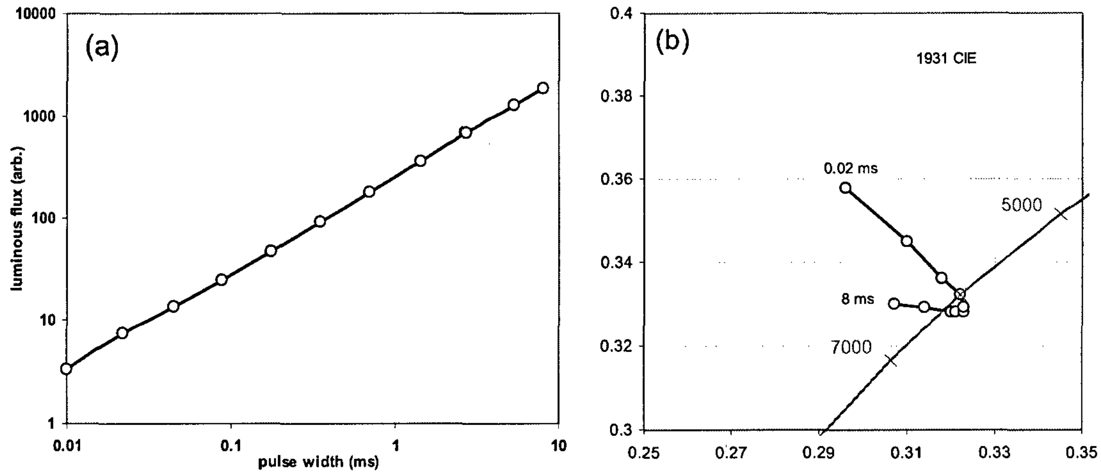

Figure 7. LED dimming: (a) variation of LED light output vs. drive pulse width at 60 Hz repetition rate; (b) variation of white-point color for same pulse widths as (a) on expanded region of CIE chart.

(PCS)[2,3] which necessarily double source area, can be used effectively. Furthermore, design of compound-parabolic concentrator[4] type integrator rods could eliminate the losses reported here for the coupling between the LED die and the light pipe, without compromising color mixing and angular control.[5,6] Doping the integrator rod with microspheres[7] could shorten the required length for adequate color mixing while eliminating the need for a separate diffuser. Thus, according to the throughput budget of Table 4, the LED/LCOS image generator could deliver 25–50% of the LED luminous output into the HMD optical system.

FACTOR	T'PUT
unpolarized source	0.50
polarization conversion	1.70
PBS Rs	0.90
PBS Tp	0.84
LCOS reflectivity	0.67
TOTAL	0.43

Table 4. Image generator optical throughput.

LED-illuminated color-sequential display systems have the advantage of equal efficiency to monochrome systems. Table 5 compares throughputs for a transmissive active-matrix liquid-crystal display (AMLCD) with those for reflective LCOS display. In the case of the transmissive AMLCD, color is produced by dividing each pixel into a triad of dots, each dot of the triad having an absorptive filter that passes light of one of the red, green, or blue primary colors. If the filters were the only loss factor, about 25% of incident white light would be passed through the red, green, and blue filters to reconstruct a white displayed image. However, the transmissive display divides the area of each pixel into an opaque fraction comprising addressing electrodes, drive transistor, and "black matrix," and a transmissive fraction. For small high-resolution color panels, as would be useful for HMD systems, the so-called pixel aperture ratio will be quite low, in the range of the 36% value we assume in Table 5. For reflective displays, the only limit on aperture ratio is how small the insulating gaps between adjacent pixel electrodes can be, resulting in ~90% aperture ratios even for high resolution panels. These factors combined give the color-sequential reflective display a 10× optical throughput advantage over a transmissive triad display. Furthermore, color-sequential displays deliver images of superior quality, as seen in Figure 8, which shows a full-frame image from a color-sequential Displaytech 432 × 240 pixel (104k pixels) electronic viewfinder (a) and close-up images from that display (b) and a competing 180k-dot AMLCD.

	TRANS. AMLCD	REFL. LCOS
technique	filter triads	LED FSC
filter t'put	25%	–
aperture	36%	90%
TOTAL	9%	90%

Table 5. Optical throughput for triad and field-sequential color (FSC) modes.

The optical efficiency and brightness achievable with HMD systems like those described here offer performance advantages for several applications. Brightness adequate for HMD use in cockpit environments with see-through to sunlit outdoor scenery could be had, even with full color. For battery-operated portable equipment, display brightness of 150 nit (50 fL) would require illuminator power of less than 4 mW. The high achievable luminous output favors HMD optical systems where imaging performance is traded for throughput. For example, the Pancake Window®-type[8] optic offers a very wide field of view with outstanding correction and long eye relief, but suffers from low optical throughput. A modern high-throughput version of this optic (NVIS, Inc, Reston, VA) uses polarization-sensitive beam

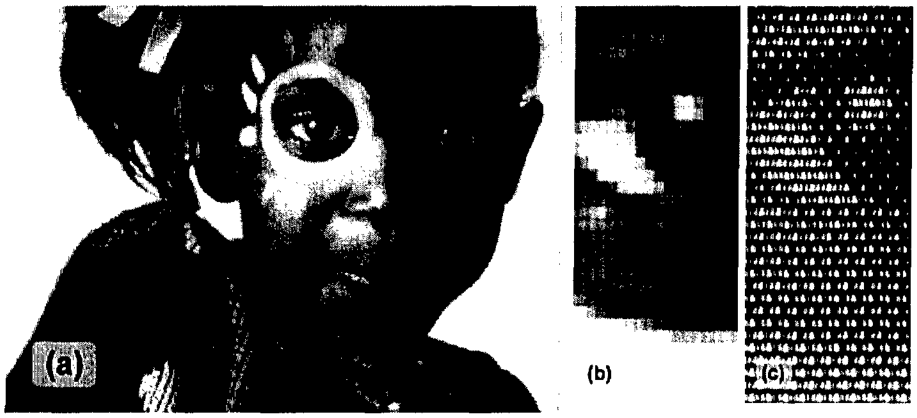

Figure 8. Display images: (a), (b) FSC LCOS; (c) AMLCD.

splitters to achieve a polarized-light throughput of about 13%. This optic gives a 55° diagonal field of view with the present 1280 × 768 microdisplay; our high-brightness illuminator produced a display image viewed through this optic with 5500 nit luminance.

6. ACKNOWLEDGEMENTS

This material is based upon work supported by the United States Air Force under Contract No. FA8650-05-M-6576. Any opinions, findings and conclusions or recommendations expressed in this material are those of the authors and do not necessarily reflect the views of the United States Air Force. The authors thank Mark Foglia of NVIS for the loan of the nVisor optic.

REFERENCES

[1] Gerhard Kuhn, Stefan Groetsch, Nicole Breidenassel, Wolfgang Schnabel, and Stefan Wallner, "A new LED light source for projection applications," in *2005 SID International Symposium Digest of Technical Papers,* Jay Morreale, ed. pp. 1702–1705 (Society for Information Display, San Jose, CA, 2005).

[2] Edward H. Stupp and Matthew S. Brennesholtz, *Projection Displays*, pp. 137–140 (John Wiley & Sons, New York, 1999).

[3] Markus Duelli, Tony McGettigan, Clark Pentico, "Integrator rod with polarization recycling functionality," in *2002 SID International Symposium Digest of Technical Papers,* Jay Morreale, ed. pp. 1078–1080 (Society for Information Display, San Jose, CA, 2002).

[4] Roland Winston, Juan C. Miñano, and Pablo Benítez, *Nonimaging Optics,* p. 50 ff. (Elsevier, New York, 2005).

[5] Thomas L. Davenport, William J. Cassarly, Thomas A. Hough, "Optimizing angle-to-area-converting, light-piping systems using surface features," in *Nonimaging Optics and Efficient Illumination Systems II*; Roland Winston, R. John Koshel, eds., Proceedings of SPIE **5942**, 29–38 (2005).

[6] Thomas L. Davenport, Thomas A. Hough, William J. Cassarly , "Optimization for efficient angle-to-area conversion in illumination systems," in *Novel Optical Systems Design and Optimization VII*; Jose M. Sasian, R. John Koshel, Paul K. Manhart, Richard C. Juergens, eds., Proceedings of SPIE **5524**, 93–100 (2004).

[7] Chris Deller, Geoff Smith, and Jim Franklin, "Colour mixing LEDs with short microsphere doped acrylic rods," Optics Express **12**, 3327 (2004).

[8] Joseph Anthony LaRussa, "Infinite optical image-forming apparatus," U. S. Patent Re. 27,356 (1972). Pancake Window is a trademark of the Farrand Optical Components and Instruments division of Ruhle Companies, Inc., Valhalla, NY.